 doi:10.20944/preprints202105.0001.v1

Article

In vitro Antioxidant Potential Evaluation of Non-Functionalized Fullerenes and Endofullerene

Ivan V. Mikheev [1,*], Madina M. Sozarukova [1,2], Dmitry Yu. Izmailov [3], Ivan E. Kareev [4], Elena V. Proskurnina [5], and Mikhail A. Proskurnin [1]

[1] Chemistry Department Analytical Chemistry Division of Lomonosov Moscow State University, Moscow 119991, Russia; mikheev.ivan@gmail.com
[2] Kurnakov Institute of General and Inorganic Chemistry, Russian Academy of Sciences, Moscow 119991, Russia; s_madinam@bk.ru
[3] Faculty of Fundamental Medicine, Lomonosov Moscow State University, Moscow 119234, Russia; dizm@mail.ru
[4] Institute of Problems of Chemical Physics of the Russian Academy of Sciences, 142432 Chernogolovka, Moscow Region, Russia; kareev@icp.ac.ru
[5] Research Centre for Medical Genetics, Moscow 115522, Russia; proskurnina@gmail.com
* Correspondence: mikheev.ivan@gmail.com; Tel.: +7(495)939-15-68 ext.101

Abstract: The antioxidant properties of unmodified aqueous fullerene dispersions (AFD) of C_{60}, C_{70}, Gd@C_{82} (in μM concentration range) were studied in the model of generation of organic radicals by 2,2′-azobis(2-amidinopropane) dihydrochloride (ABAP) and luminol. Purification protocols for AFDs are proposed. Based on chemiluminescence (CL) measurements, the concentration-dependent of the CL signal for any AFDs is revealed. Suppression of CL signals is up to 5 times better than Mexidol® antioxidant. The concentration of half-suppression increased in row C_{60}<C_{70}<Gd@C_{82}. We further demonstrated mathematical modeling of the long-term kinetics data for C_{60}, C_{70}, Gd@C_{82} allowed fitting of CL curves. Kinetic schemes are proposed, and the constants of each reaction are estimated (~n×μ$M^{-1}$$min^{-1}$). C_{60}, C_{70}, and Gd@C_{82} exhibit a quenching mechanism that is not an antioxidant effect. For C_{60} and C_{70}, similar behavior is shown that is not quantitatively different in kinetic modeling. On the contrary, Gd@C_{82} has a double action: (1) quenching and (2) actual antioxidant action. Estimating quenching constants for all of the AFD types showed the same magnitude. Moreover, the antioxidant activity in Gd@C_{82} is 300 times greater than in the case of C_{60} and C_{70}.

Keywords: fullerene; endofullerene; aqueous fullerene dispersion; antioxidant potential; kinetic chemiluminometry

1. Introduction

Water-soluble fullerenes are promising candidates for different medical applications, and they have been proposed as vital components for humans and environmental systems [1]. Fullerenes, in particular, their water-soluble derivatives are considered as radical scavenging agents [2], possess antioxidant activity [3], acquire remarkable antimicrobial properties [4], cytotoxicity [5], DNA cleavage, and lipid peroxidation mediated by reactive oxygen species (ROS) [6]. As for non-functionalized aqueous dispersions (AFD) (without addends) [7], their antioxidant and superoxide anion-radical (SAR) scavenging properties have not been thoroughly studied. First attempts at study superoxide dismutase (SOD) mimic activity have yet been made [8] *in vitro* and cell models. It is known that unsaturated lipids are a target of free radicals. The mechanism of their oxidation (lipid peroxidation) has been described and proved [6]. The result is the accumulation of lipid hydroperoxides, intermediate stable products. The ability of fullerenes to initiate lipid oxidation has not been widely assessed before. There is a slight report on their ability to trap lipid peroxyl radicals and act as chain-breaking antioxidants [9]. The impact of fullerenes in *in*

 doi:10.20944/preprints202105.0001.v1

vivo and *in vitro* experiments for *Cyprinus carpio* brains confirmed the absence of lipid peroxidation [10].

Recent reviews discussed [11] that fullerenes possess an inert scaffold with antioxidant functionalities. Biologically active water-soluble fullerene adducts are also discussed in [12]. C_{60} is an extremely weak chain-breaking antioxidant with an inherent rate constant for trapping peroxyl radicals per se (k_{inh}=0.3×10^3 $M^{-1}s^{-1}$). However, some antioxidants covalently bound to fullerenes increase antioxidant activity insignificantly. Grafting their surface with small-molecule antioxidants such as synthetic phenols (2,6-di-tert-butyl-4-methylphenol) broadens their antioxidant behavior conveying peroxyl radical-trapping activity up to 30 times [13]. C_{60} conjugated with phenols indicates a significant improvement of oxidative stability [14]. A C_{60} derivative with covalently bonded (an analog of α-tocopherol with hydroxychromanyl moiety) is an effective antioxidant acting in two model lipid matrices: saturated stearic acid and unsaturated linolenic acid during the non-isothermal oxidation tested by differential scanning calorimetry [15]. There is an ambiguity in information about the ability of fullerenes to generate ROS. Several studies deals with C_{60} solutions stimulating ROS generation [16]. Another study evidenced the antioxidative properties of fullerenes [17].

The conventional approach to describing the antioxidant properties of low molecular weight free radical scavengers is based on quantitative determination of their ability to terminate free radical chain reactions, relatively a standard antioxidant compound. Evaluation of the antioxidant status of compounds, the total radical-trapping potential (TRAP) method, and total antioxidant reactivity (TAR) from luminol-enhanced chemiluminescence (CL) measurements is previously developed [18]. This approach is based on the ability to trap radicals formed during the decomposition of thermolabile azo compounds in radical-induced reactions. However, this technique does not consider the individual physicochemical characteristics of the antioxidant. A more rigorous approach to the description of antioxidant properties considers the determination of the antioxidant concentration and the mathematical modeling estimation [19] of the rate constant of the interaction with the radicals [20]. Different antioxidants possess different chemiluminescence curves, making it impossible to use any universal parameter to characterize the amount or activity of antioxidants of different chemical nature [21].

Fullerene soot C_{60} and C_{70} not only retards oxidation in the mode of an alkyl radical quencher but also operates as a peroxy radical scavenger [22] in the model reaction of initiated (2,2′- azobisisobutyronitrile, AIBN). For reactivity of C_{60} during oxidation of a series of hydrocarbons shows that the fullerene does not react with the RO_2• radicals indicate an extremely weak rate constant estimated from CL [23].

Of fundamental importance is had the functional fullerenes derivatives, but it is beyond the scope of this article to study these derivatives. There are almost no works related to the study of antioxidant properties in the generation of organic radicals for unmodified fullerenes. As far as we are concerned, no one has ever used kinetics modeling for fullerenes to assess the interception ability of radicals. This paper reports data on the antioxidant properties of aqueous fullerene dispersions. Using computer simulation, prediction of the rate constants and the reaction scheme has been proposed.

2. Results

2.1. Aqueous Fullerenes Material Safety Data Sheet

In this study, ultrasound-assisted preparation of AFD for pristine C_{60}, C_{70}, $Gd@C_{82}$ was used. The AFD showed excellent stability for more than 20 months; all of the information about the characterization of AFD was previously published elsewhere [7]. The main drawback of this process is an accumulation of titanium dioxide nanoparticles (TiO_2 NPs) due to cavitation sonotrode erosion. It is confirmed by ICP-OES analysis for metal impurities in AFDs (

Table 1).

Preprints (www.preprints.org) | NOT PEER-REVIEWED | Posted: 3 May 2021 doi:10.20944/preprints202105.0001.v1

Table 1. Elemental composition of fullerene dispersions after preparation by direct ultrasound probe sonication (during 5h short-time duty) checked by inductively coupled plasma atomic emission spectroscopy (ICP-OES). Slurry sampling introduction in ICP-OES spectrometer. All results uncertainty were ± 15%.

Type of AFD or number of compounds	Syringe filter type	$c_{Fullerene}$, ppm	pH*	*c*, ppb																			
				Ag	Al	As	B	Ba	Be	Cd	Co	Cr	Cu	Fe	Li	Mn	Mo	Ni	Pb	Si	Ti	V	Zn
C_{60}	Pristine AFD (no filter using)	1210 ± 50	7.35	<5	290	<5	320	17	<0.1	25	<1	<1	80	75	16	45	273	60	<1	2530	595	32	29
	450 nm	260 ± 20	7.44	<5	<10	<5	105	<1	<0.1	<0.5	<1	<1	7	7	2	5	10	<1	<1	1620	<1	<1	6
	220 nm	90 ± 10	7.40	<5	<10	<5	105	<1	<0.1	<0.5	<1	<1	7	7	2	4	10	4	<1	1600	<1	2.4	6
	Combination of 450 and 220 nm filter	280 ± 24	7.45	<5	<10	<5	105	<1	<0.1	<0.5	<1	<1	7	7	2	4	<5	3	<1	1650	2.3	<1	6
C_{70}	450 nm	120 ± 10	7.55	<5	<10	<5	90	<1	<0.1	<0.5	<1	<1	5	5	2	2	<5	<1	<1	1520	<1	<1	<2
$Gd@C_{82}$	450 nm	20 ± 4	7.74**	<5	<10	<5	12	<1	<0.1	<0.5	<1	<1	2	8	2	2	<5	<1	<1	1450	<1	<1	<2

*, uncertainty was ± 0.10 pH units;

**, pH of pristine AFD $Gd@C_{82}$ was 7.89.

Preprints (www.preprints.org) | NOT PEER-REVIEWED | Posted: 3 May 2021 doi:10.20944/preprints202105.0001.v1

A syringe polyvinylidene fluoride (PVDF) filter has been used to remove particles from AFDs. The filter removes large fullerene nanoparticles (more than 1 μm) and finally cleans titanium nanoparticles (less *ca*. 1 ppb) from the ultrasonic probe. The ICP-OES showed that AFDs contain silicon, which cannot be removed by syringe filtering.

2.2. *Scavenger Antioxidant Properties in The Model of ABAP Decay*

We studied the antioxidant properties of AFDs by activated kinetic chemiluminescence in a molecular model of organic radical generation is thermal-induced decomposition of 2,2'-azobis(2-amidinopropane)dihydrochloride (ABAP) in the presence of luminol. Based on the data obtained, we evaluated the antioxidant capacity and mathematical modeling of the reaction kinetics (see below). A common antioxidant, Trolox® [24], was used as a standard comparison substance. Also, to compare the behavior of fullerenes in the ABAP system in the presence of luminol, we compared the behavior with the medium strength antioxidant, Mexidol® [25].

The shape of the analytical CL signal for Trolox (100 and 200 nM) is shown in Figure 1.

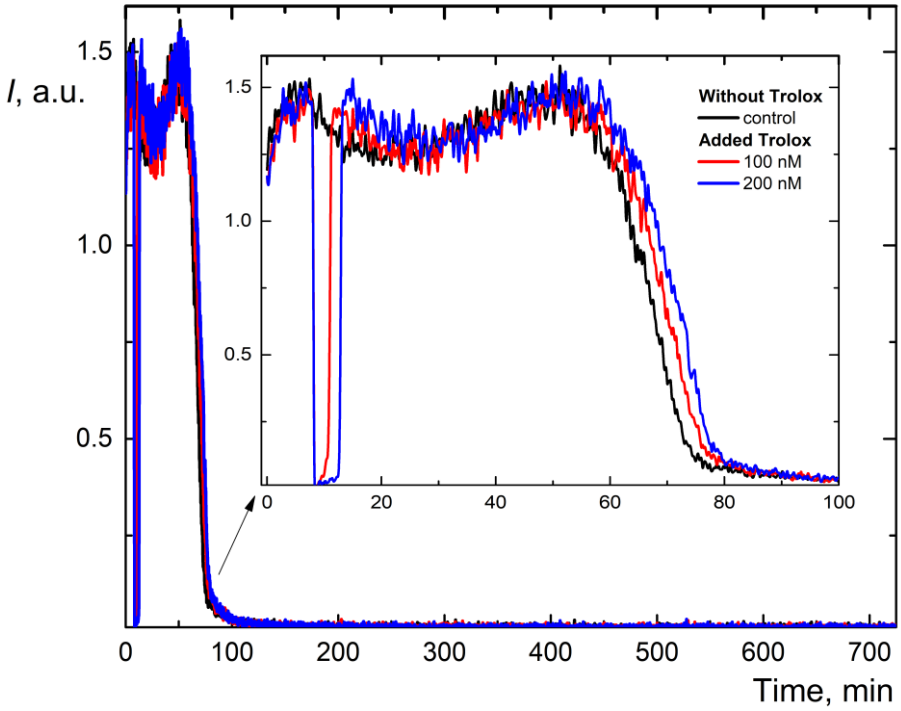

Figure 1. Long-term chemiluminograms of strong antioxidant Trolox® in the system 2.5 mM ABAP and 2 μM luminol up to 725 min, the enlarged area corresponds to a time of up to 100 minutes.

The shape of the analytical signal for Mexidol (10÷50 μM) is shown in Figure 2.

Preprints (www.preprints.org) | NOT PEER-REVIEWED | Posted: 3 May 2021 doi:10.20944/preprints202105.0001.v1

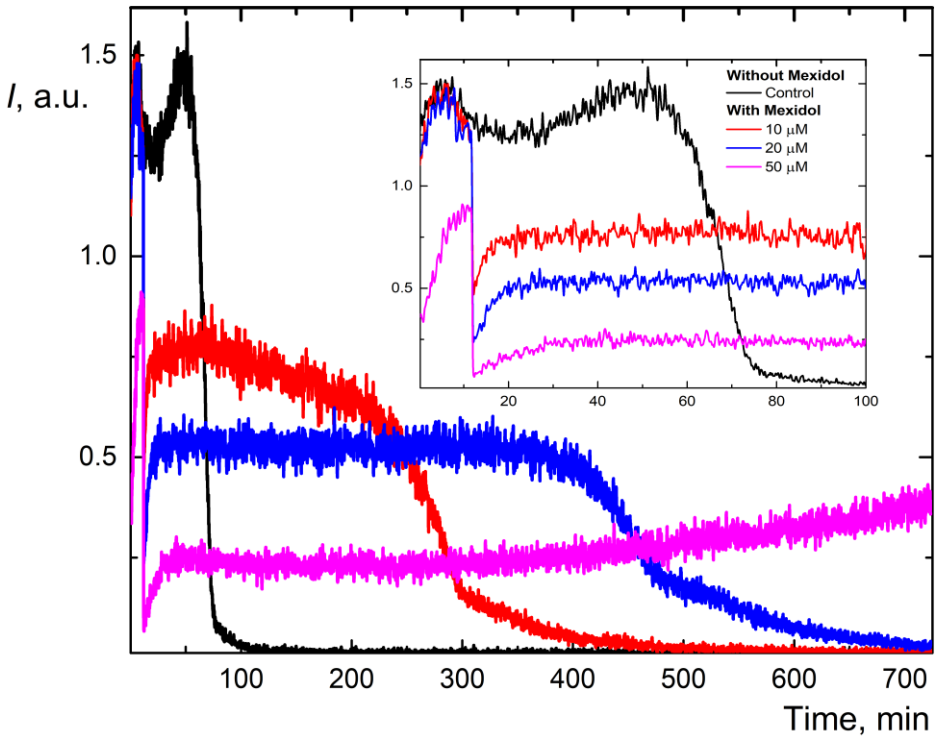

Figure 2. Long-term chemiluminograms of medium-capacity antioxidant, Mexidol® in the system 2.5 mM ABAP and 2 μM luminol up to 725 min, the enlarged area corresponds to a time of up to 100 minutes.

The signal behavior of the chemiluminogram in Figure 1 is typical for strong antioxidants; different curves were obtained for AFDs Figure 3, 4, 5.

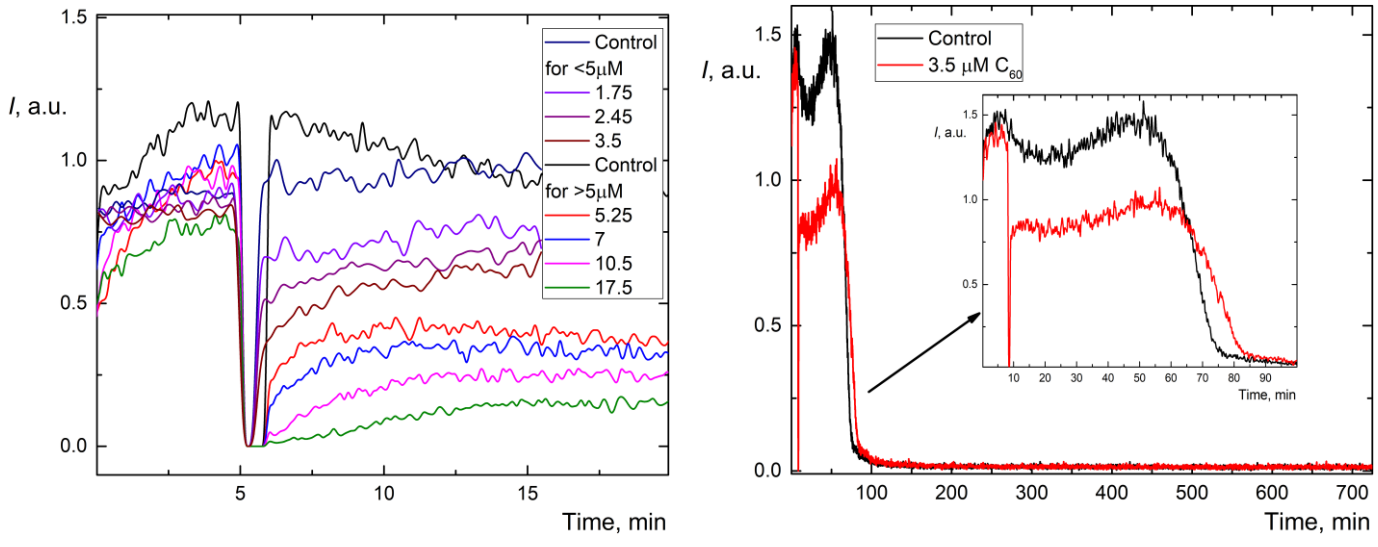

(**a**) (**b**)

Figure 3. (a) Chemiluminograms of aqueous fullerene C_{60} dispersions in a range of concentration 1.8÷18 μM in the system 2.5 mM ABAP and 2 μM luminol up to 20 min; (b) Long-term chemiluminograms of aqueous fullerene C_{60} dispersions (3.5 μM) in the system 2.5 mM ABAP and 2 μM luminol up to 725 min, the enlarged area corresponds to a time of up to 100 minutes.

Preprints (www.preprints.org) | NOT PEER-REVIEWED | Posted: 3 May 2021 doi:10.20944/preprints202105.0001.v1

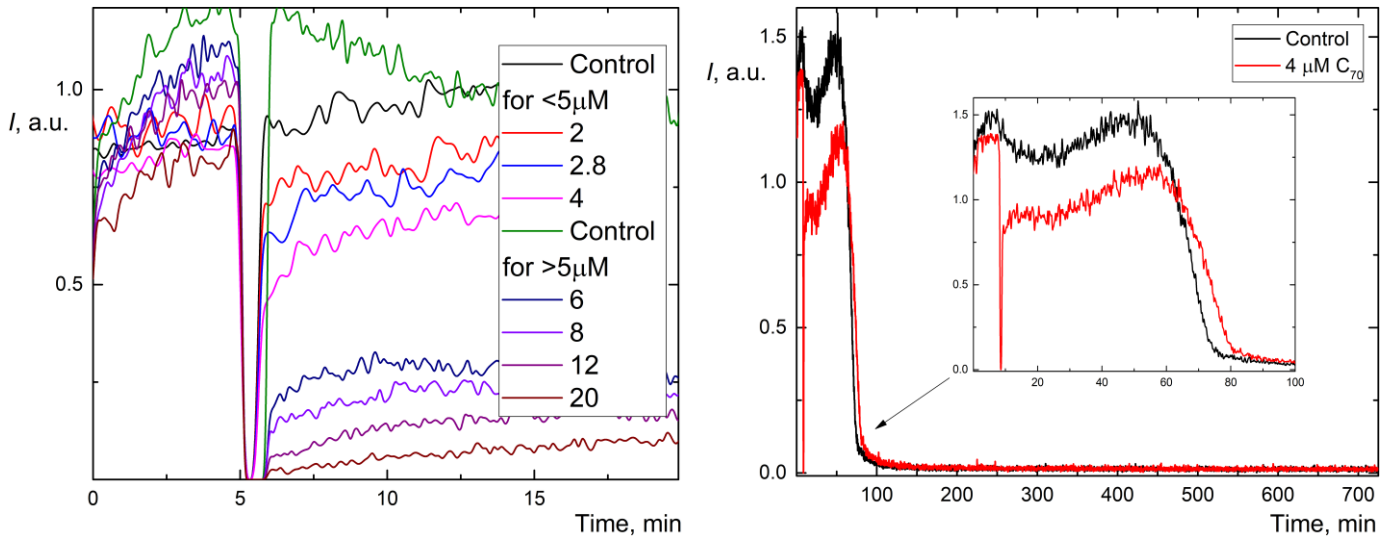

(**a**) (**b**)

Figure 4. (a) Chemiluminograms of aqueous fullerene C_{70} dispersions in a range of concentration 2.0÷20 μM in the system 2.5 mM ABAP and 2 μM luminol up to 20 min; (b) Long-term chemiluminograms of aqueous fullerene C_{70} dispersions (4.0 μM) in the system 2.5 mM ABAP and 2 μM luminol up to 725 min, the enlarged area corresponds to a time of up to 100 minutes.

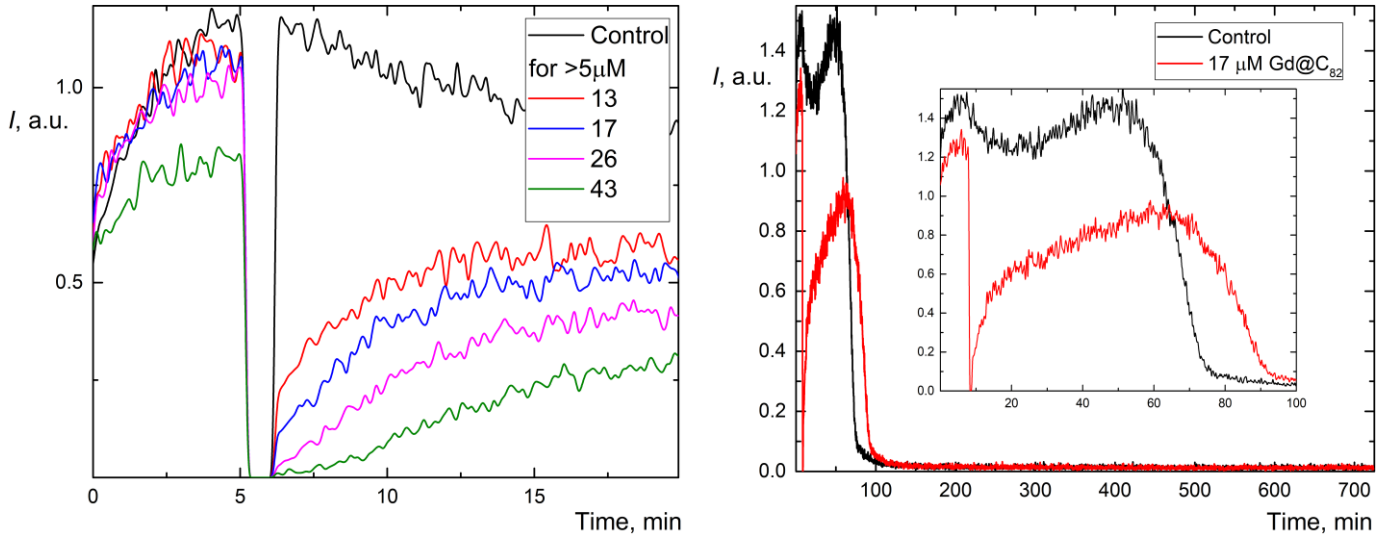

(**a**) (**b**)

Figure 5. (a) Chemiluminograms of aqueous fullerene Gd@C_{82} dispersions in a range of concentration 4.0÷40 μM in the system 2.5 mM ABAP and 2 μM luminol up to 20 min; (b) Long-term chemiluminograms of aqueous fullerene Gd@C_{82} dispersions (17 μM) in the system 2.5 mM ABAP and 2 μM luminol up to 725 min, the enlarged area corresponds to a time of up to 100 minutes.

The shape of the analytical signal suppression, in this case, coincides with the shape of the curves for medium-strength antioxidants. The general form of chemiluminescence diagrams for all AFDs in the narrow (up to 20 min) and long time intervals (up to 720 min) is presented for C_{60} at Figure 3, C_{70} at Figure 4, Gd@C_{82} at Figure 5.

The calculated characteristics of the antioxidant strength for Mexidol and AFDs are shown in Table 2. It is shown that AFDs can be ranked by their ability to suppress chemiluminescence as $C_{60} > C_{70} > Gd@C_{82}$. Ratios of half-suppression signal concentrations were 1:1.7:3.5.

Preprints (www.preprints.org) | NOT PEER-REVIEWED | Posted: 3 May 2021 doi:10.20944/preprints202105.0001.v1

2.3. Computer Simulation of The Fullerene Aqueous Dispersions Antioxidant Activity (Complete chemiluminescence kinetics before antioxidant depletion)

The use of rate constants of the inhibition reaction can be used as an indicator of antioxidant activity. We recorded the kinetics of chemiluminescence for mathematical modeling of antioxidant action to the moment of depletion (disappearance) of the antioxidant, ~100 min. Dependences for standard substances are shown in Figure 1, 2, for AFDs, in Figure 3b, 4b, and 5b. Experimental and calculated curves have a sufficient degree of coincidence. The effect of the strong antioxidant, Trolox, on CL kinetics is expressed in the complete suppression of CL (a "latent period" [26]); depletion of the antioxidant is characterized by an increase in the intensity of CL and return to the previous stationary (control) level. Thus, for the Trolox concentration of 200 nM, the latent period was ~3.5 sec, the time of radical depletion in the system is ~90 min (Figure 1). In contrast, the effect of Mexidol shows that for concentrations of ~10 μM, the effect of complete signal suppression occurs at more than 400 min, with an increase in concentration to 20 μM this period is >700 min.

For the AFDs in the long-term experiment, the experimental curves recorded the moment of antioxidant depletion, which for all types of AFDs was from 85 to 100 minutes (Figure 3b, 4b, and 5b). In this regard, it is possible to compare the mathematical model and experimental data for all AFD types studied in this work. To carry out the kinetics simulation, we selected the optimum concentration ranges of the investigated AFDs (Table 2).

Table 2. Estimation of half-maximal inhibitory concentration for aqueous fullerene dispersions (AFD). n=5, P=0.95. pH in all cases stabilized by using phosphate buffer solution 0.1 M KH_2PO_4.

Compound	Range of investigated fullerene concentration, μM	Linear fit	$c_{1/2}$, μM
Mexidol®	10÷50	S=–(67.7 ± 6.2)×$c_{Mexidol}$+4354 ± 167, r=–0.9918	30.8 ± 1.0
C_{60}	1.8÷18	S=–(75.8 ± 6.0)×c_{Ful}+973 ± 16, r=–0.9955	6.4 ± 0.3
C_{70}	2.0÷20	S=–(46.2 ± 2.0)×c_{Ful}+1006 ± 23, r=–0.9956	11.0 ± 0.4
Gd@C_{82}	4.0÷40	S=–(28.4 ± 4.5)×c_{Ful}+1335 ± 76, r=–0.9754	22.6 ± 0.8

We also chose the most suitable exact concentration values for which we observed a suppression of CL intensity ~2 times. From the experimental data presented, all AFDs satisfy the requirements necessary for mathematical modeling:

(1) the moment of antioxidant depletion is registered;
(2) the concentration dependence is traced.

The experimental and model dependences for AFD C_{60} (Figure 6a), C_{70} (Figure 6b), and Gd@C_{82} (Figure 6c) are shown below.

Preprints (www.preprints.org) | NOT PEER-REVIEWED | Posted: 3 May 2021 doi:10.20944/preprints202105.0001.v1

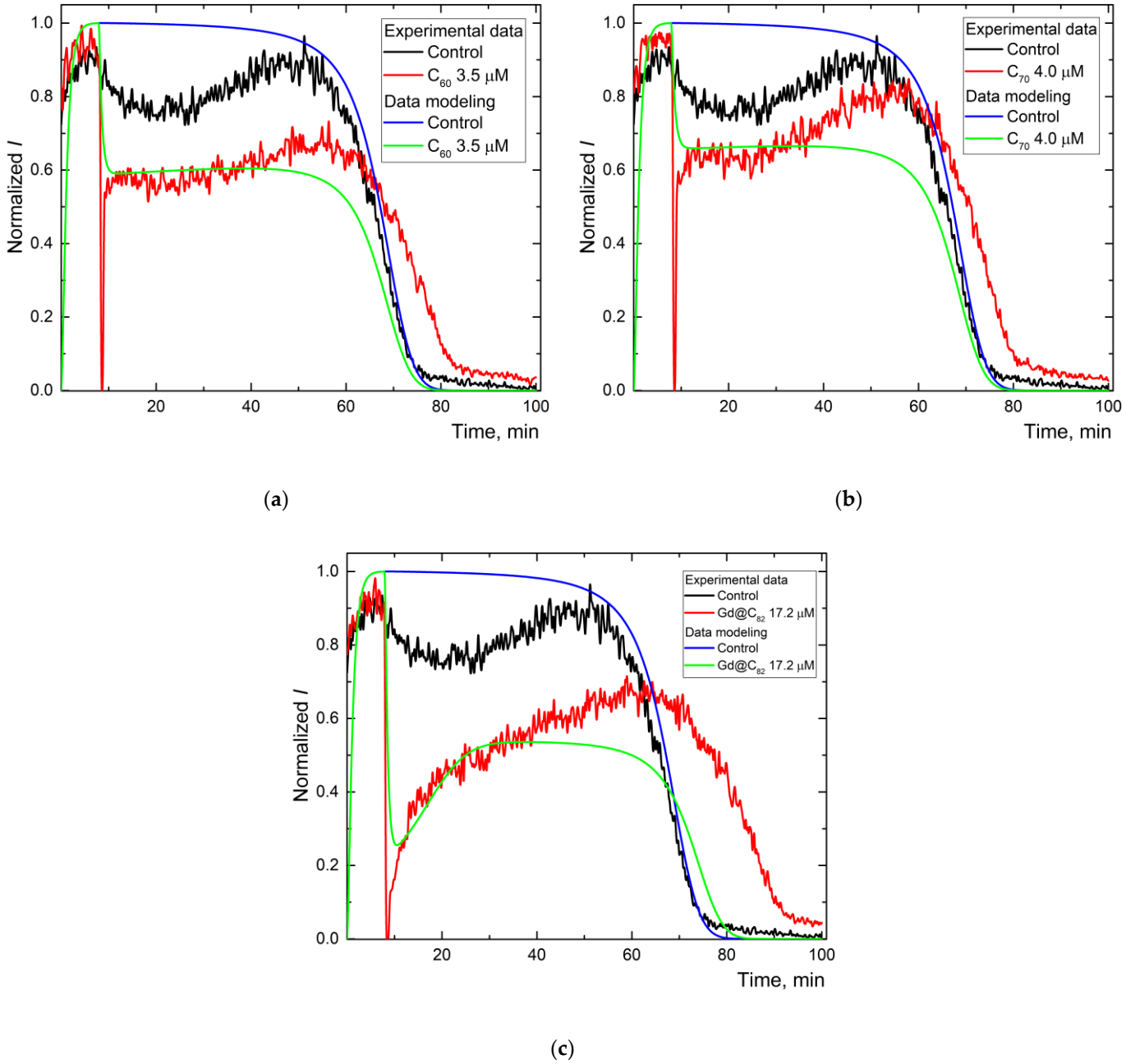

Figure 6. The experimental and simulated chemiluminescence plots for aqueous fullerene dispersions C_{60} (a), C_{70} (b), Gd@C_{82} (c) for one-stage mechanism. In all cases, solid lines have a specific color: black is the control experiment, blue is the modeling data of the control experiment, red is experimental data for aqueous fullerene dispersions, green is modeling data for aqueous fullerene dispersions.

A simple mathematical model was used to simulate the steady-state level of chemiluminescence (without adding antioxidants), whose kinetic scheme consisted of two reactions:

(1) the free radical generation reaction from ABAP;
(2) chemiluminescence reactions.

Combined reaction schemes:

1) ABAP → R• (constant k_R), decomposition of ABAP
2) R• + Lum → RLum* (constant k_{Lum}), formation of the excited product
2a) RLum* → P + hν luminescence

Preprints (www.preprints.org) | NOT PEER-REVIEWED | Posted: 3 May 2021 doi:10.20944/preprints202105.0001.v1

where R• is a free radical or reaction product in the electronically excited state, which reacts with the antioxidants, P is the stable product of the free-radical reaction.

To model the action of antioxidants, reactions with fullerenes (3) were added to reactions (1), (2, 2a):

3) $AO_1 + RLum^* \rightarrow ...$ (constant k_{In1})

3a) $AO_2 + R \rightarrow ...$ (constant k_{In2})

Reaction (3), which is general for all AFDs, was included in all kinetic schemes. The principle is the interaction of AFDs with the excited product of luminol. For more coincidence of experimental and model data only in the AFD Gd@C_{82} reaction (3a), intercepting obtained radicals from ABAP was added. An acceptable match between the experimental CL data and the mathematical modeling data for AFDs C_{60}, C_{70}, Gd@C_{82} was obtained under the following conditions (Table 3).

Table 3. Initial simulation conditions for on-stage mechanism in case of C_{60} and C_{70}, and two-stage for Gd@C_{82}

Initial concentrations, μM	Type of modeling systems					Name of substances
	ABAP	C_{60}	C_{70}	Gd@C_{82}	Trolox®	
ABAP	2500					ABAP
R	0					Radical of ABAP
Lum	2					Luminol
$RLum^*$	0					Excited product
AO_1	n/a	3.5	4.0	17.2	0, 0.1, 0.2	Antioxidant 1
AO_2	n/a	n/a	n/a	0.172	n/a	Antioxidant 2
Reactions	Value of simulated constant, $\mu M^{-1}min^{-1}$					Type of free-radical reactions
ABAP → R	1.25				1.7	ABAP decomposition
R + Lum → $RLum^*$	2					Formation of an excited product
$RLum^* \rightarrow P + h\nu$	1				4	Luminescence
$AO_1 + RLum^* \rightarrow ...$	n/a	0.20	0.13	0.13	10000	Antioxidant reaction 1
$AO_2 + R \rightarrow ...$	n/a	n/a	n/a	30	n/a	Additional reaction

n/a — not applied

Thus, it is possible to arrange AFDs in a sequence by strength $C_{60} > C_{70} \sim$ Gd@C_{82}, the ratio of reaction rate constants between antioxidant (AFD) and free radical for C_{60}, C_{70}, and Gd@C_{82} are 1.5:1:1.

3. Discussion

Since the priority of this work is to model the process kinetics and a deeper understanding of the mechanism of the process, we did the steps below.

(1) Chemiluminescent systems can be influenced by the purity of the AFDs objects under study. Moreover, the action of the impurity component can be taken as a false positive mechanism, so we carried out a deep purification of the AFDs (as in the section above). Thus, eliminating the influence of this factor.

(2) Fullerenes are known to be both antioxidants [27], possess fluorescence [28], and act as fluorescence quenchers [29,30]. Therefore, we preliminarily evaluated the properties of fullerenes as quenchers and showed that AFDs act as quenchers for the (a) ABAP and luminol system and (b) only luminol presence. The order of the Stern–Volmer quenching constants coincides with the existing data (see Supplementary Materials).

 doi:10.20944/preprints202105.0001.v1

3.1. Peculiarities of Preparation Procedure and Aqueous Fullerene Dispersions Purification

Our experience with the implementation of the sonication system for the preparation of carbonaceous nanomaterials (hydrosols of nanodiamond) reveals titanium impurities [31] even for a short time (e.g., several minutes) of ultrasound treatment. Ti accumulation rate was proportional to the prolonged ultrasound exposure time [32].

Our previous experiments proved that titanium and silicon are in the form of oxide [8]. However, processes of purification of AFD would not be resolved by now. It is associated with transition metal (TM)–carbon interactions [33]. It is essential to choose the right filter system. We suggest using commercially available syringe PVDF membrane filters 0.22 or 0.45 μm. PVDF membrane can be attributed to the high affinity of TiO_2 for water [34]; the presence of hydroxyl moieties from TiO_2 NPs contributed to improving the hydrophilicity, thereby improving the water flux [35]. As shown in

Table 1, filtration with a 0.22 or 0.45 μm PVDF filter completely removes TiO_2 NPs fullerene dispersions.

Moreover, [32] showed that 0.2 μm PTFE filter has low filtration efficiency from titanium. This is due to redox reactions between TiO_2 NPs and Pu(III)/Pu(IV) at low pH solutions. However, for practically neutral AFDs

Table 1, the efficiency of using PVDF filters is high. The presence of impurities can reduce or increase the effectiveness of antioxidants. The ability of TiO_2 NPs to enhance the production of SAR and alter the antioxidant system in human osteoblast cells is shown in [36]. As well impurities may adversely affect the reproducibility of results [37]. To evaluate the efficiency of fullerene antioxidant capacity, preparation of pure dispersion is an essential item.

As for SiO_2 NPs, it remains in solution (approximately 65%, see

Preprints (www.preprints.org) | NOT PEER-REVIEWED | Posted: 3 May 2021 doi:10.20944/preprints202105.0001.v1

Table 1) after filtration using PVDF filters. In [38] showed that SiO_2 NPs pass through the membrane during filtering with polytetrafluoroethylene (PTFE) membranes in a range 0.1–1.0 μm of pore size. In our opinion, we find a residual silica content due to:

(1) Typically silica SiO_2 NPs can be formed with less 220 nm in diameter [39];

Intermolecular and intramolecular interactions deal with

(2) Probable silica surface with an adsorbed fullerene monolayer [40];

(3) Sorption SiO_2 NPs on the surface of fullerene [41].

The addition of SiO_2 NPs increased the capacity of the antioxidant enzymes superoxide dismutase (SOD), catalase (CAT), glutathione reductase (GR), and phenylalanine ammonia-lyase (PAL) in plants [42]. In our work, the total content of SiO2 NPs is less than the total fullerene content ratio in-stock solution from 10 to 170 times, which remains diluted. Therefore, it should not affect the enhancement of antioxidant activity. The study of such a mechanism was beyond the scope of this work.

3.2. Antioxidant Activity in the System of Generation of Organic Radicals and Simulations of chemiluminescence kinetic for aqueous fullerene dispersions

Analysis showed that the data on the activity of unmodified fullerenes and their aqueous dispersions are practically absent. The closest fullerene derivatives in the structure are fullerenols, which have up to 42 hydroxyl groups in their structure, depending on the type of fullerene in the series from C_{60} to $Gd@C_{82}$. Hydroxylation is one of the cheapest and most straightforward approaches to dissolving fullerenes in water and does not require deep purification of the resulting product. However, it should not be excluded that the appearance of even minor surface derivatization can lead to an increase in the antioxidant activity of fullerenes [43]. It was shown that [44] less toxicity and greater antioxidant capacity is proven for fullerenols $C_{60}O_y(OH)_x$, $C_{60,70}O_y(OH)_x$, x+y=24÷28. There are two limitations of using any derivatization of fullerene surface they are related to the fact that:

(1) additional groups can be involved in metabolic processes, groups on the surface can reduce the availability of the π-electron system, leading to reversible free radical capture [45], differently affect the spin environment [46];

(2) fullerene derivatives could act as potent oxidizing agents under excitation with light in the presence of oxygen [47].

We only studied AFDs C_{60}, C_{70}, and $Gd@C_{82}$ without addends in our work. Moreover, first of all, we proceeded to the comparison of known antioxidant systems. Measurements of the antioxidant action of Mexidol are used to calibrate the chemiluminescence dependences for determining the level of free radical generation. For bioluminescence and chemiluminescence, half-maximum signal suppression concentration is widely used to assess the overall fullerene toxicity and antioxidant properties [44]. Moreover, the half-maximum signal suppression concentration for fullerenes is 1.5 to 5.0 times lower than Mexidol, which shows their better antioxidant activity. Comparison of fullerenes with each other shows an increase in the level of half-maximum signal suppression concentration for AFD in the series ($c_{1/2}$ C_{60}<C_{70}<$Gd@C_{82}$) this is because the proportion of "active" fullerene molecules decreases in the series C_{60}>C_{70}>$Gd@C_{82}$. Previously, we showed [8] that the fraction of active molecules on the surface (% of total concentration) is 1.6 : 1.5 : 0.9, which agrees with the obtained chemiluminescence suppression series in the organic radical generation model.

From the presented experimental data for fullerenes, we can make a preliminary conclusion (without mathematical modeling) that the antioxidant activity (relative radical interception rate) of fullerenes differs insignificantly (within one order). A significant difference shown in the antioxidant capacity is the number of intercepted radicals per 1 particle of a substance. In order to simulate the kinetics of reactions, the whole CL curve was recorded to establish the moment of antioxidant depletion. This effect is seen in the convergence of chemiluminescence curves: (a) control experiment (without antioxidant) and (b) with antioxidant. This point is very crucial for testing the mathematical model. In the experiment and the mathematical model, the antioxidant should run out after the same

 doi:10.20944/preprints202105.0001.v1

time after addition. If the moment of antioxidant depletion is not registered in the experimental data, it is impossible to assert the adequacy of the mathematical model parameters.

Antioxidant rate constants allow us to discriminate fullerenes by antioxidant strength. AFDs C_{60} and C_{70} are weak antioxidants and approximately equal in strength; Gd@C_{82} exhibits two antioxidant components. Numerically AFDs C_{60} appeared slightly more active antioxidant than C_{70}, as for Gd@C_{82} activity is comparable with C_{70}. In [48] classified the strength of antioxidants according to constants obtained from process kinetics simulations, strong antioxidants from 2000 $nM^{-1}min^{-1}$, medium-strength from 100 $nM^{-1}min^{-1}$, and weak ones below 10 $nM^{-1}min^{-1}$. The C_{60}, C_{70}, and Gd@C_{82} constants obtained in Table 3 are comparable and refer to medium strength antioxidants. As shown in Table 3, the added concentration of Gd@C_{82} was 4 times higher than C_{70} and C_{60} (17.2 and ~4 μM, respectively). For these initial conditions, the effect of the 2nd antioxidant contained in Gd@C_{82} was evident. Moreover, the content of the 2nd antioxidant was 100 times less, while the activity was about 300 times higher. The 2nd antioxidant in Gd@C_{82} is characterized by a different mechanism of action dealing with the interception of ABAP radicals rather than quenching of excited luminol molecules. AFDs C_{60} and C_{70} likely contain such an antioxidant, but their action is little noticeable due to their low concentration.

AFDs turned out to be very weak antioxidants; they do not give a latent period, as in the strong antioxidant Trolox [48]. Also, the fullerene in AFDs differ from Mexidol in the mechanism of action:

(1) Mexidol intercepts degradable ABAP radicals;
(2) On the contrary, fullerenes C_{60}, C_{70}, and Gd@C_{82} intercept the excited product of luminol. There is the quenching of chemiluminescence, rather than competition with luminol molecules for free radicals, seen by the magnitude of the constant values (Table 3).

This part of the quenching mechanism and the role of fullerenes in reducing the fluorescence signal are still unclear [49]. In some cases, it has been shown that fullerenes and fullerenols can non-covalently bind molecules, exhibiting dynamic luminescence quenching, for example, with Ribonuclease A [50]. However, the binding sites in each case are individual; for a more detailed study of the system and the nature of the binding, molecular dynamics simulations should be performed [51]. In additional experiments (see Supporting Information), we evaluated the luminescence quenching constants for the ABAP and luminol mixture studied, as well as for luminol alone. In both cases, we observed comparable orders of magnitude values of Stern-Volmer quenching constants for C_{60}, C_{70}, Gd@C_{82}: $C_{70} > C_{60} > Gd@C_{82}$.

This data can be explained by the polarizability (α) of the fullerene molecules for C_{60} and C_{70}. The more significant efficiency of the quenching of the electronically excited states by the C_{70} can be attributed to the higher average polarizability of the C_{70} molecule [52]. The polarizability is for the C_{60} (82.7 $Å^3$) and C_{70} (102.7 $Å^3$) [53], Gd@C_{82} 114.67 $Å^3$ [54] at that $\alpha_{EMF} < \alpha_{atom} + \alpha_{Fullerene}$. In addition, (1) the reactivity upon A_E-type reactions for the fullerenes decreased in the order C_{60} > Gd@C_{82} [55]; (2) C_{82} is a better free radical scavenger than C_{60}, the presence of endoatoms improves the fullerenes antiradical capacity [56].

However, a 1.3-fold decrease in the quenching constants for Gd@C_{82} could explain a different behavior in the chemiluminescence reaction, a change in the quenching mechanism to a bimolecular one [57], or the involvement of the molecule in another competing process at multiple positions of the fullerene cage [55]. Thus, according to the kinetic simulation results, we obtained:

(3) The Gd@C_{82} AFDs have a tiny amount of "true antioxidant" admixture. In general, for Gd@C_{82}, we observe the same background process of action as quenchers. However, on the other hand, we obtain an antioxidant effect based on calculations based on chemiluminescence curves (order of constants in mathematical modeling) and the experimental course of the curves. From the simulation, we can conclude that the effect is comparable to Mexidol, which intercepts exactly ABAP

 doi:10.20944/preprints202105.0001.v1

radicals, but because of the primary and predominant action of CL quenching, it is pretty difficult to separate and measure the signals.

On the other hand, the different behavior for $Gd@C_{82}$ AFD can be explained by (1) the presence of a carbon frame that contains the inner paramagnetic metal ion Gd^{3+} with spin S=7/2, (2) the presence of anion $Gd@C_{82}^{3-}$ acting as a radical located on the outer shell [58]. $Gd@C_{82}^{3-}$ can involve in free-radical addition reaction, which can change the electronic structure of the inner cluster and subsequently affect its configuration [59]. The electron affinity values of $Gd@C_{82}$ are more significant than those for pristine C_{60} and C_{70} (1.25 and 1.19 times greater for $Gd@C_{82}$). It can be indicated that $Gd@C_{82}$ can act as a strong electron donor and an electron acceptor [60].

4. Materials and Methods

4.1. Aqueous fullerene dispersions preparations

Preparation and complete characterization techniques for aqueous fullerene dispersions were recently described elsewhere [7]. In this work, we used long-term stable AFD of the pristine: (1) C_{60}, (2) C_{70} (NeoTechProduct LLC (Russia), 99+% HPLC-grade); (3) the enriched soot containing the $Gd@C_{2n}$ EMFs (total content of Gd atoms up to 4 wt. % has been synthesized by the evaporation of the composite graphite electrodes compounded by gadolinium in the electric arc reactor as we previously described [61].

4.2. Techniques and additional reagents

The enhanced chemiluminescence protocol for quantification of the antioxidant activity of aqueous fullerene dispersions C_{60}, C_{70}, and $Gd@C_{82}$ has been used. The chemiluminescent system consisted of a source of free radicals cationic 2,2′-azobis (2-amidinopropane) dihydrochloride (ABAP) (Sigma, USA) and a chemiluminescent probe 5-Amino-2,3-dihydrophthalazine-1,4-dione (Luminol) (Sigma, USA). A luminol solution of 1 mM (Sigma, USA) and ABAP solution of 50 mM were prepared by dissolving the weighed samples in phosphate buffer solution 0.1 M KH_2PO_4 at pH 7.4 (Sigma, USA). The overall volume in a PC (polycarbonate) cuvette was 1.00 mL in all experiments. The stock solution of ABAP (2.5 mM) and luminol (2 μM) in the mixture were added to a buffer solution (pH 7.4) at 37°C.

Reference antioxidant compound: Trolox® (±)-6-Hydroxy-2,5,7,8-tetra-methylchromane-2-carboxylic acid (Sigma, USA); Mexidol® ethylmethylhydroxypyridine succinate 50 mg/ml solution for intravenous and intramuscular administration (LLC "NPK" PHARMASOFT", Russia). The chemiluminescence signal was recorded up to achieving stationary level, and then an aliquot of the antioxidant solution of Trolox or AFDs was added. The registration was performed until the novel steady-state level was reached.

4.3. *Equipment*

The measurements were carried out with a Lum-1200 chemiluminometer with 12-channel (DISoft, Russia). The chemiluminometer makes available visible light detection within a range from 300 to 700 nm. No bandpass filters were used. Signal processing was performed via PowerGraph 3.3 Professional software (DISoft, Russia). The relative standard deviation of chemiluminescence intensity did not exceed 0.05. Fluorolog®-2 spectrofluorimeter (Horiba Jobin Yvon, Japan) was used. The statistical processing of the data was performed with STATISTICA v.10.0 software (StatSoft Inc., USA).

4.4. Auxiliary equipment

Millex-HV Syringe Filter Unit, 0.22 and 0.45 μm, hydrophilic PVDF, 33 mm, non-sterilized were used for AFD filtration during the preparation process (Millipore, Germany). Sartorius Proline Plus (Germany) mechanical pipettor single-channel 10÷100, 100÷1000 μL were used for graduation and preparation of solutions, which calibrated by ISO 8655-2:2002. The ultrasound probe MEF93.T (LLC MELFIZ-ul'trazvuk, Russia) working in a continuous mode of exposure to ultrasonic energy at operating frequency 22.00 ± 1.65 kHz

Preprints (www.preprints.org) | NOT PEER-REVIEWED | Posted: 3 May 2021 doi:10.20944/preprints202105.0001.v1

has been used for AFD preparation. pH-meter SevenCompact™ pH/Ion S220 (Mettler-Toledo AG, Switzerland) was used to prepare phosphate buffer solution. According to IUPAC recommendation [62], calibration was performed using NIST Traceable standard buffer solutions with pH 1.68, 4.01, 6.68, 9.18, 11.00 (Hanna Instruments, USA).

4.5. Computer simulation and data handling

The computer simulation was carried out with the specially designed computer program "Kinetic Analyzer" (by Dr. D. Izmailov). For a set of the predetermined reactions and the initial concentrations of the reactants, the rate constants were selected, providing the maximal curve fitting of experimental and calculated plots. As a criterion for maximal curve fitting, the minimum sum of squared residuals was calculated with the OriginPro 2015 software (OriginLab, USA).

As an analytical signal characterizing the antioxidant capacity of AFD was the difference between the intensities of stationary chemiluminescence level $\Delta I = I_0 - I$ (Figure 7). This parameter linearly depended on the concentration of added AFD.

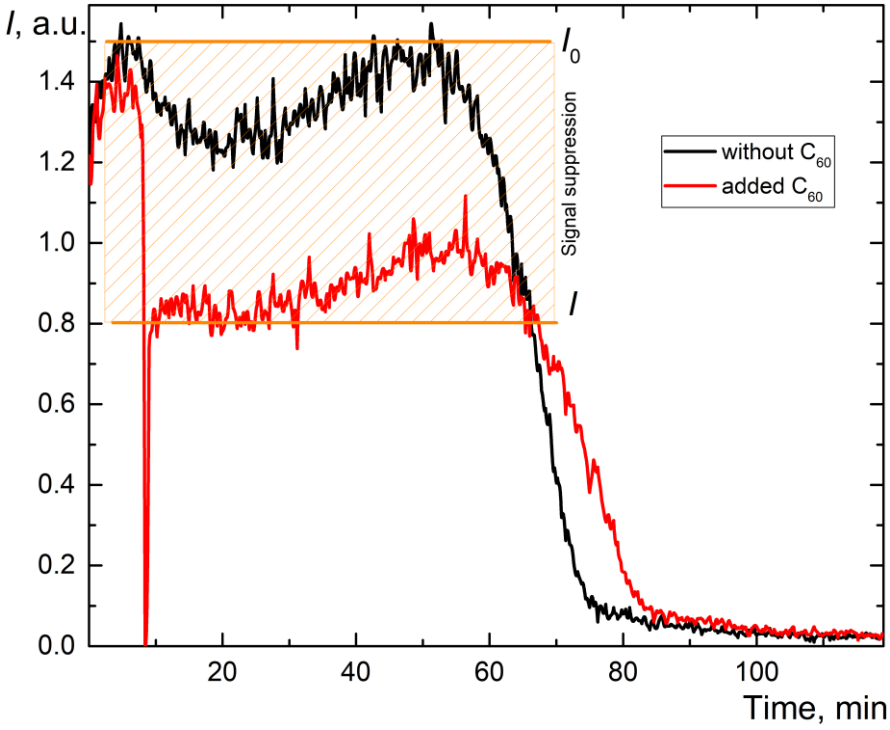

Figure 7. The shape of analytical signal (ΔI) suppression by aqueous fullerene dispersions characterizing the antioxidant capacity. ΔI is a difference between the intensities of the stationary level without suppression (I_0) and with aqueous fullerene dispersions spike (I).

Chemiluminograms in the molecular model of generation of organic radicals for C_{60}, C_{70}, Gd@C_{82} were used to determine the concentration of half-suppression of the chemiluminescent signal for all AFDs ($c_{1/2}$, μM). The concentration of half-suppression of luminescence ($c_{1/2}$, μM) is a concentration that reduces the amplitude of the signal (ΔI) or the light sum of the signal (S) of the response by two times and can hypothetically be taken as a quantitative indicator of the inhibitory activity of a given compound.

5. Conclusions

This paper is the first work to evaluate the antioxidant activity of fullerenes, which will be helpful in further evaluation of antioxidant properties in a living cell. C_{60}, C_{70}, Gd@C_{82} AFDs show no antioxidant activity in the system of organic radical-induced ABAP decay. We prove that it is not free radical capture but quenching. In the case of

Gd@C_{82}, there is a show of significant antioxidant effect. The results provide insights into the possible mechanism of interactions of fullerenes between free-radicals C_{60}, C_{70}, Gd@C_{82}, which are of fundamental importance for understanding the potential biomedical effects of AFDs.

We believe that this work will help create reference materials for further study of the antioxidant properties of functional fullerene derivatives. To create such platforms, AFDs of C_{60}, C_{70}, Gd@C_{82} can be proposed as model substances not exhibiting antioxidant properties. Also, the absence of a significant free radical interception effect allows the development of sensors to control impurity composition, acting as a free radical interceptor rather than as a quencher for *in vitro* and *in vivo* experiments.

Supplementary Materials: The following are available online at www.mdpi.com/xxx/s1, Figure S1, S2: The fluorescent spectra of aqueous fullerene dispersions C_{60}, C_{70}, and Gd@C_{82} act as a quencher at different systems ABAP+luminol, and only luminol.

Author Contributions: Conceptualization, E.V.P. and M.A.P.; methodology, E.V.P. and M.A.P.; software, D.Y.I.; validation, I.V.M. and M.M.S..; formal analysis, I.V.M. and M.M.S.; investigation, I.V.M. and M.M.S.; resources, I.E.K.; data curation, I.V.M.; writing—original draft preparation, I.V.M.; writing—review and editing, E.V.P. and M.A.P.; visualization, I.V.M.; supervision, E.V.P. and M.A.P.; project administration, M.A.P.; funding acquisition, I.V.M. All authors have read and agreed to the published version of the manuscript.

Funding: The Russian Science Foundation has supported this work under Contract No. 19-73-00143. This research was performed according to the Development program of the Interdisciplinary Scientific and Educational School of Lomonosov Moscow State University, «The future of the planet and global environmental change».

Acknowledgments: V.P. Bubnov, who provided the technical support for Gd-endofullerene synthesis.

Conflicts of Interest: The authors declare no conflict of interest.

References

1. Colvin, V.L. The potential environmental impact of engineered nanomaterials. *Nature Biotechnology* **2003**, *21*, 1166-1170, doi:10.1038/nbt875.

2. Yu, C.; J.B., B.; Taizoon, C.; Jen-Pang, H.; Jentaie, S.; Bo-Ji, C.; Y., C.L. Novel Water-soluble Hexa(sulfobutyl)fullerenes as Potent Free Radical Scavengers. *Chemistry Letters* **1998**, *27*, 465-466, doi:10.1246/cl.1998.465.

3. Witte, P.; Beuerle, F.; Hartnagel, U.; Lebovitz, R.; Savouchkina, A.; Sali, S.; Guldi, D.; Chronakis, N.; Hirsch, A. Water solubility, antioxidant activity and cytochrome C binding of four families of exohedral adducts of C60 and C70. *Organic & Biomolecular Chemistry* **2007**, *5*, 3599-3613, doi:10.1039/B711912G.

4. Pellarini, F.; Pantarotto, D.; Da Ros, T.; Giangaspero, A.; Tossi, A.; Prato, M. A Novel [60]Fullerene Amino Acid for Use in Solid-Phase Peptide Synthesis. *Organic Letters* **2001**, *3*, 1845-1848, doi:10.1021/ol015934m.

5. Cheng, F.; Yang, X.; Fan, C.; Zhu, H. Organophosphorus chemistry of fullerene: synthesis and biological effects of organophosphorus compounds of C60. *Tetrahedron* **2001**, *57*, 7331-7335.

6. Kamat, J.; Devasagayam, T.; Priyadarsini, K.; Mohan, H. Reactive oxygen species mediated membrane damage induced by fullerene derivatives and its possible biological implications. *Toxicology* **2000**, *155*, 55-61.

7. Mikheev, I.V.; Pirogova, M.O.; Usoltseva, L.O.; Uzhel, A.S.; Bolotnik, T.A.; Kareev, I.E.; Bubnov, V.P.; Lukonina, N.S.; Volkov, D.S.; Goryunkov, A.A.; et al. Green and rapid preparation of long-term stable aqueous dispersions of fullerenes and endohedral fullerenes: The pros and con of an ultrasonic probe. *Ultrasonics Sonochemistry* **2021**, 105533, doi:https://doi.org/10.1016/j.ultsonch.2021.105533.

8. V. Mikheev, I.; M. Sozarukova, M.; V. Proskurnina, E.; E. Kareev, I.; A. Proskurnin, M. Non-Functionalized Fullerenes and Endofullerenes in Aqueous Dispersions as Superoxide Scavengers. *Molecules* **2020**, *25*, 2506.

9. Grebowski, J.; Konopko, A.; Krokosz, A.; DiLabio, G.A.; Litwinienko, G. Antioxidant activity of highly hydroxylated fullerene C60 and its interactions with the analogue of α-tocopherol. *Free Radical Biology and Medicine* **2020**, *160*, 734-744, doi:https://doi.org/10.1016/j.freeradbiomed.2020.08.017.

10. Shinohara, N.; Matsumoto, T.; Gamo, M.; Miyauchi, A.; Endo, S.; Yonezawa, Y.; Nakanishi, J. Is Lipid Peroxidation Induced by the Aqueous Suspension of Fullerene C60 Nanoparticles in the Brains of Cyprinus carpio? *Environmental Science & Technology* **2009**, *43*, 948-953, doi:10.1021/es802182f.

11. Valgimigli, L.; Baschieri, A.; Amorati, R. Antioxidant activity of nanomaterials. *Journal of Materials Chemistry B* **2018**, *6*, 2036-2051, doi:10.1039/C8TB00107C.

12. Sharoyko, V.V.; Ageev, S.V.; Podolsky, N.E.; Petrov, A.V.; Litasova, E.V.; Vlasov, T.D.; Vasina, L.V.; Murin, I.V.; Piotrovskiy, L.B.; Semenov, K.N. Biologically active water-soluble fullerene adducts: Das Glasperlenspiel (by H. Hesse)? *Journal of Molecular Liquids* **2021**, *323*, 114990, doi:https://doi.org/10.1016/j.molliq.2020.114990.

13. Enes, R.F.; Tomé, A.C.; Cavaleiro, J.A.S.; Amorati, R.; Fumo, M.G.; Pedulli, G.F.; Valgimigli, L. Synthesis and Antioxidant Activity of [60]Fullerene–BHT Conjugates. *Chemistry – A European Journal* **2006**, *12*, 4646-4653, doi:https://doi.org/10.1002/chem.200501495.

14. Czochara, R.; Kusio, J.; Litwinienko, G. Fullerene C60 conjugated with phenols as new hybrid antioxidants to improve the oxidative stability of polymers at elevated temperatures. *RSC Advances* **2017**, *7*, 44021-44025, doi:10.1039/C7RA08764K.

15. Czochara, R.; Grajda, M.; Kusio, J.; Litwinienko, G. Expanding the antioxidant activity into higher temperatures—Fullerene C60 conjugated with α-Tocopherol analogue as a hybrid antioxidant in saturated lipid systems. *Bulg. Chem. Commun* **2018**, *50*, 268-274.

16. Wang, C.; Lin, Y.; Wang, Y.; Liang, Y.; Meng, L.; Zhang, J.; Zhou, Q.; Jiang, G. Induced temperature-dependent DNA degradation by C60 without photoactivation. *Chinese Science Bulletin* **2011**, *56*, 3100, doi:10.1007/s11434-011-4694-6.

17. Wang, I.C.; Tai, L.A.; Lee, D.D.; Kanakamma, P.P.; Shen, C.K.F.; Luh, T.-Y.; Cheng, C.H.; Hwang, K.C. C60 and Water-Soluble Fullerene Derivatives as Antioxidants Against Radical-Initiated Lipid Peroxidation. *J. Med. Chem.* **1999**, *42*, 4614-4620, doi:10.1021/jm990144s.

18. Lissi, E.; Salim-Hanna, M.; Pascual, C.; del Castillo, M.D. Evaluation of total antioxidant potential (TRAP) and total antioxidant reactivity from luminol-enhanced chemiluminescence measurements. *Free Radical Biology and Medicine* **1995**, *18*, 153-158, doi:https://doi.org/10.1016/0891-5849(94)00117-3.

19. Magin, D.V.; Izmaĭlov, D.; Popov, I.N.; Levin, G.; Vladimirov Iu, A. [Photochemiluminescent study of the antioxidant activity in biological systems. Mathematical modeling]. *Voprosy meditsinskoi khimii* **2000**, *46*, 419-425.

20. Vladimirov, Y.A.; Proskurnina, E.V.; Izmajlov, D.Y. Kinetic chemiluminescence as a method for study of free radical reactions. *Biophysics* **2011**, *56*, 1055-1062, doi:10.1134/S0006350911060200.

21. Sozarukova, M.M.; Shestakova, M.A.; Teplonogova, M.A.; Izmailov, D.Y.; Proskurnina, E.V.; Ivanov, V.K. Quantification of Free Radical Scavenging Properties and SOD-Like Activity of Cerium Dioxide Nanoparticles in Biochemical Models. *Russian Journal of Inorganic Chemistry* **2020**, *65*, 597-605, doi:10.1134/S0036023620040208.

22. Zeynalov, E.B.; Allen, N.S.; Salmanova, N.I. Radical scavenging efficiency of different fullerenes C60–C70 and fullerene soot. *Polymer Degradation and Stability* **2009**, *94*, 1183-1189, doi:https://doi.org/10.1016/j.polymdegradstab.2009.04.027.

23. Bulgakov, R.G.; Ponomareva, Y.G.; Maslennikov, S.I.; Nevyadovsky, E.Y.; Antipina, S.V. Inertness of C60 fullerene toward RO2 • peroxy radicals. *Russian Chemical Bulletin* **2005**, *54*, 1862-1865, doi:10.1007/s11172-006-0049-x.

24. Boulebd, H. Comparative study of the radical scavenging behavior of ascorbic acid, BHT, BHA and Trolox: Experimental and theoretical study. *Journal of Molecular Structure* **2020**, *1201*, 127210, doi:https://doi.org/10.1016/j.molstruc.2019.127210.

25. Jian, C.e.; Yan, J.; Zhang, H.; Zhu, J. Recent advances of small molecule fluorescent probes for distinguishing monoamine oxidase-A and monoamine oxidase-B in vitro and in vivo. *Molecular and Cellular Probes* **2021**, *55*, 101686, doi:https://doi.org/10.1016/j.mcp.2020.101686.

26. Lissi, E.; Pascual, C.; Del Castillo, M.D. Luminol Luminescence Induced by 2,2′-Azo-Bis(2-Amidinopropane) Thermolysis. *Free Radical Research Communications* **1992**, *17*, 299-311, doi:10.3109/10715769209079523.

27. Gharbi, N.; Pressac, M.; Hadchouel, M.; Szwarc, H.; Wilson, S.R.; Moussa, F. [60]Fullerene is a Powerful Antioxidant in Vivo with No Acute or Subacute Toxicity. *Nano Letters* **2005**, *5*, 2578-2585, doi:10.1021/nl051866b.

28. Catalan, J.; Elguero, J. Fluorescence of fullerenes (C60 and C70). *Journal of the American Chemical Society* **1993**, *115*, 9249-9252, doi:10.1021/ja00073a046.

29. Campbell, K.; Zappas, A.; Bunz, U.; Thio, Y.S.; Bucknall, D.G. Fluorescence quenching of a poly(para-phenylene ethynylenes) by C60 fullerenes. *Journal of Photochemistry and Photobiology A: Chemistry* **2012**, *249*, 41-46, doi:https://doi.org/10.1016/j.jphotochem.2012.08.015.

30. Liu, B.M.; Zhang, J.; Hao, A.J.; Xu, L.; Wang, D.; Ji, H.; Sun, S.J.; Chen, B.Q.; Liu, B. The increased binding affinity of curcumin with human serum albumin in the presence of rutin and baicalin: A potential for drug delivery system. *Spectrochimica Acta - Part A: Molecular and Biomolecular Spectroscopy* **2016**, *155*, 88-94, doi:10.1016/j.saa.2015.11.010.

31. Myasnikov, I.Y.; Gopin, A.V.; Mikheev, I.V.; Chernysheva, M.G.; Badun, G.A. Presonication of nanodiamond hydrosols in radiolabeling by a tritium thermal activation method. *Mendeleev Communications* **2018**, *28*, 495-496, doi:https://doi.org/10.1016/j.mencom.2018.09.014.

32. Virot, M.; Venault, L.; Moisy, P.; Nikitenko, S.I. Sonochemical redox reactions of Pu(iii) and Pu(iv) in aqueous nitric solutions. *Dalton Transactions* **2015**, *44*, 2567-2574, doi:10.1039/C4DT02330G.

33. Kiciński, W.; Dyjak, S. Transition metal impurities in carbon-based materials: Pitfalls, artifacts and deleterious effects. *Carbon* **2020**, *168*, 748-845, doi:https://doi.org/10.1016/j.carbon.2020.06.004.

34. Martins, P.M.; Miranda, R.; Marques, J.; Tavares, C.J.; Botelho, G.; Lanceros-Mendez, S. Comparative efficiency of TiO2 nanoparticles in suspension vs. immobilization into P(VDF–TrFE) porous membranes. *RSC Advances* **2016**, *6*, 12708-12716, doi:10.1039/C5RA25385C.

35. Samree, K.; Srithai, P.-u.; Kotchaplai, P.; Thuptimdang, P.; Painmanakul, P.; Hunsom, M.; Sairiam, S. Enhancing the Antibacterial Properties of PVDF Membrane by Hydrophilic Surface Modification Using Titanium Dioxide and Silver Nanoparticles. *Membranes* **2020**, *10*, 289.

36. Niska, K.; Pyszka, K.; Tukaj, C.; Wozniak, M.; Radomski, M.W.; Inkielewicz-Stepniak, I. Titanium dioxide nanoparticles enhance production of superoxide anion and alter the antioxidant system in human osteoblast cells. *Int J Nanomedicine* **2015**, *10*, 1095-1107, doi:10.2147/IJN.S73557.

37. Apak, R.; Özyürek, M.; Güçlü, K.; Çapanoğlu, E. Antioxidant Activity/Capacity Measurement. 1. Classification, Physicochemical Principles, Mechanisms, and Electron Transfer (ET)-Based Assays. *Journal of Agricultural and Food Chemistry* **2016**, *64*, 997-1027, doi:10.1021/acs.jafc.5b04739.

38. Ullmann, C.; Babick, F.; Stintz, M. Microfiltration of Submicron-Sized and Nano-Sized Suspensions for Particle Size Determination by Dynamic Light Scattering. *Nanomaterials* **2019**, *9*, 829.

39. Kimoto, S.; Dick, W.D.; Hunt, B.; Szymanski, W.W.; McMurry, P.H.; Roberts, D.L.; Pui, D.Y.H. Characterization of nanosized silica size standards. *Aerosol Science and Technology* **2017**, *51*, 936-945, doi:10.1080/02786826.2017.1335388.

40. Davydov, V.Y.; Sheppard, N.; Osawa, E. An Infrared Spectroscopic Study of the Hydrogenation and Dehydrogenation of the Complexes of Aromatic Compounds and of Fullerene C60 with Silica-Supported Platinum. *Journal of Catalysis* **2002**, *211*, 42-52, doi:https://doi.org/10.1006/jcat.2002.3694.

41. Chen, K.L.; Elimelech, M. Interaction of Fullerene (C60) Nanoparticles with Humic Acid and Alginate Coated Silica Surfaces: Measurements, Mechanisms, and Environmental Implications. *Environmental Science & Technology* **2008**, *42*, 7607-7614, doi:10.1021/es8012062.

42. Emamverdian, A.; Ding, Y.; Mokhberdoran, F.; Xie, Y.; Zheng, X.; Wang, Y. Silicon dioxide nanoparticles improve plant growth by enhancing antioxidant enzyme capacity in bamboo (Pleioblastus pygmaeus) under lead toxicity. *Trees* **2020**, *34*, 469-481, doi:10.1007/s00468-019-01929-z.

43. Sachkova, A.S.; Kovel, E.S.; Churilov, G.N.; Guseynov, O.A.; Bondar, A.A.; Dubinina, I.A.; Kudryasheva, N.S. On mechanism of antioxidant effect of fullerenols. *Biochemistry and Biophysics Reports* **2017**, *9*, 1-8, doi:https://doi.org/10.1016/j.bbrep.2016.10.011.

44. Kovel, E.S.; Sachkova, A.S.; Vnukova, N.G.; Churilov, G.N.; Knyazeva, E.M.; Kudryasheva, N.S. Antioxidant Activity and Toxicity of Fullerenols via Bioluminescence Signaling: Role of Oxygen Substituents. *International Journal of Molecular Sciences* **2019**, *20*, 2324.

45. Eropkin, M.Y.; Melenevskaya, E.Y.; Nasonova, K.V.; Bryazzhikova, T.S.; Eropkina, E.M.; Danilenko, D.M.; Kiselev, O.I. Synthesis and Biological Activity of Fullerenols with Various Contents of Hydroxyl Groups. *Pharmaceutical Chemistry Journal* **2013**, *47*, 87-91, doi:10.1007/s11094-013-0901-x.

46. Zhou, S.; Yamamoto, M.; Briggs, G.A.D.; Imahori, H.; Porfyrakis, K. Probing the Dipolar Coupling in a Heterospin Endohedral Fullerene–Phthalocyanine Dyad. *Journal of the American Chemical Society* **2016**, *138*, 1313-1319, doi:10.1021/jacs.5b11641.

47. Hamblin, M.R. Fullerenes as photosensitizers in photodynamic therapy: pros and cons. *Photochemical & Photobiological Sciences* **2018**, *17*, 1515-1533, doi:10.1039/C8PP00195B.

48. Proskurnina, E.V.; Izmailov, D.Y.; Sozarukova, M.M.; Zhuravleva, T.A.; Leneva, I.A.; Poromov, A.A. Antioxidant Potential of Antiviral Drug Umifenovir. *Molecules* **2020**, *25*, 1577.

49. Sluch, M.; Samuel, I.; Petty, M. Quenching of pyrene fluorescence by fullerene C60 in Langmuir–Blodgett films. *Chemical physics letters* **1997**, *280*, 315-320.

50. Roy, P.; Bag, S.; Chakraborty, D.; Dasgupta, S. Exploring the Inhibitory and Antioxidant Effects of Fullerene and Fullerenol on Ribonuclease A. *ACS Omega* **2018**, *3*, 12270-12283, doi:10.1021/acsomega.8b01584.

51. McHedlov-Petrossyan, N.O. Fullerenes in Liquid Media: An Unsettling Intrusion into the Solution Chemistry. *Chemical Reviews* **2013**, *113*, 5149-5193, doi:10.1021/cr3005026.

52. Bulgakov, R.G.; Galimov, D.I.; Sabirov, D.S. New property of the fullerenes: the anomalously effective quenching of electronically excited states owing to energy transfer to the C70 and C60 molecules. *JETP Letters* **2007**, *85*, 632-635, doi:10.1134/S0021364007120090.

53. Compagnon, I.; Antoine, R.; Broyer, M.; Dugourd, P.; Lermé, J.; Rayane, D. Electric polarizability of isolated C 70 molecules. *Physical Review A* **2001**, *64*, 025201.

54. Zakharova, A.V.; Bedrina, M.E. A quantum chemical study of endometallofullerenes: Gd@C70, Gd@C82, Gd@C84, and Gd@C90. *The European Physical Journal D* **2020**, *74*, 116, doi:10.1140/epjd/e2020-10109-5.

55. Wang, Z.; Lu, Z.; Zhao, Y.; Gao, X. Oxidation-induced water-solubilization and chemical functionalization of fullerenes C60, Gd@C60 and Gd@C82: atomistic insights into the formation mechanisms and structures of fullerenols synthesized by different methods. *Nanoscale* **2015**, *7*, 2914-2925, doi:10.1039/C4NR06633B.

56. Andrade, E.-B.; Martínez, A. Free radical scavenger properties of metal-fullerenes: C60 and C82 with Cu, Ag and Au (atoms and tetramers). *Computational and Theoretical Chemistry* **2017**, *1115*, 127-135, doi:https://doi.org/10.1016/j.comptc.2017.06.015.

57. Liu, X.; Ying, X.; Li, Y.; Yang, H.; Hao, W.; Yu, M. Identification differential behavior of Gd@C82(OH)22 upon interaction with serum albumin using spectroscopic analysis. *Spectrochimica Acta Part A: Molecular and Biomolecular Spectroscopy* **2018**, *203*, 383-396, doi:https://doi.org/10.1016/j.saa.2018.05.125.

58. Furukawa, K.; Okubo, S.; Kato, H.; Shinohara, H.; Kato, T. High-Field/High-Frequency ESR Study of Gd@C82-I. *The Journal of Physical Chemistry A* **2003**, *107*, 10933-10937, doi:10.1021/jp035947c.

59. Fang, H.; Cong, H.; Suzuki, M.; Bao, L.; Yu, B.; Xie, Y.; Mizorogi, N.; Olmstead, M.M.; Balch, A.L.; Nagase, S.; et al. Regioselective Benzyl Radical Addition to an Open-Shell Cluster Metallofullerene. Crystallographic Studies of Cocrystallized Sc3C2@Ih-C80 and Its Singly Bonded Derivative. *Journal of the American Chemical Society* **2014**, *136*, 10534-10540, doi:10.1021/ja505858y.

60. Guha, S.; Nakamoto, K. Electronic structures and spectral properties of endohedral fullerenes. *Coordination Chemistry Reviews* **2005**, *249*, 1111-1132, doi:https://doi.org/10.1016/j.ccr.2004.11.017.

61. Bubnov, V.P.; Laukhina, E.E.; Kareev, I.E.; Koltover, V.K.; Prokhorova, T.G.; Yagubskii, E.B.; Kozmin, Y.P. Endohedral metallofullerenes: A convenient gram-scale preparation. *Chemistry of Materials* **2002**, *14*, 1004-1008, doi:10.1021/cm011106b.

62. Buck, R.P.; Rondinini, S.; Covington, A.K.; Baucke, F.G.K.; Brett, C.M.A.; Camoes, M.F.; Milton, M.J.T.; Mussini, T.; Naumann, R.; Pratt, K.W.; et al. Measurement of pH. Definition, standards, and procedures (IUPAC Recommendations 2002). *Pure and Applied Chemistry* **2002**, *74*, 2169-2200, doi:doi:10.1351/pac200274112169.